Characterization of vasopressin V2 receptor mutants in nephrogenic diabetes insipidus in a polarized cell model

J. H. Robben, N. V. A. M. Knoers and P. M. T. Deen

Am J Physiol Renal Physiol 289:F265-F272, 2005. doi:10.1152/ajprenal.00404.2004

AJP - Renal Physiology publishes original manuscripts on a broad range of subjects relating to the kidney, urinary tract, and their respective cells and vasculature, as well as to the control of body fluid volume and composition. It is published 12 times a year (monthly) by the American Physiological Society, 9650 Rockville Pike, Bethesda MD 20814-3991. ISSN: 1931-857X, ESSN: 1522-1466. Visit our website at http://www.the-aps.org/.

Am J Physiol Renal Physiol 289: F265–F272, 2005;
doi:10.1152/ajprenal.00404.2004.

TRANSLATIONAL PHYSIOLOGY

Characterization of vasopressin V2 receptor mutants in nephrogenic diabetes insipidus in a polarized cell model

J. H. Robben,[1] N. V. A. M. Knoers,[2] and P. M. T. Deen[1]

[1]*Department of Physiology, Nijmegen Centre for Molecular Life Sciences, and* [2]*Department of Human Genetics, Radboud University Nijmegen Medical Centre, Nijmegen, The Netherlands*

Submitted 9 November 2004; accepted in final form 9 March 2005

Robben, J. H., N. V. A. M. Knoers, and P. M. T. Deen. Characterization of vasopressin V2 receptor mutants in nephrogenic diabetes insipidus in a polarized cell model. *Am J Physiol Renal Physiol* 289: F265–F272, 2005; doi:10.1152/ajprenal.00404.2004.—X-linked nephrogenic diabetes insipidus (NDI) is caused by mutations in the gene encoding the vasopressin V2 receptor (V2R). For the development of a tailored therapy for NDI, knowledge of the cellular fate of V2R mutants is needed. It would be useful when this fate could be predicted from the location and type of mutation. To identify similarities and differences in localization, maturation, stability, and degradation of COOH-terminal GFP-tagged V2R mutants, we stably expressed nine mutants in polarized Madin-Darby canine kidney cells. The mutants V2R-L44P, -Δ62–64, -I130F, -S167T, -S167L, and -V206D were mainly expressed in the endoplasmic reticulum (ER) as immature proteins. These mutants had relatively short half-lives due to proteasomal degradation, except for V2R-Δ62–64. In contrast, V2R-R113W, -G201D, and -T204N were expressed in the ER and in the basolateral membrane as immature, high-mannose glycosylated, and mature complex-glycosylated proteins. The immature forms of V2R-R113W and -T204N, but not V2R-G201D, were rapidly degraded. The mature forms varied extensively in their stability and were degraded by only lysosomes (V2R-T204N and wild-type V2R) or lysosomes and proteasomes (V2R-G201D, -R113W). These data reveal that most missense V2R mutations lead to retention in the ER and suggest that mutations that likely distort a transmembrane domain or introduce a charged amino acid close to it make a V2R mutant more prone to ER retention. Because six of the mutants tested showed significant increases in intracellular cAMP levels on transient expression in COS cells, activation of these six receptors following rescue of cell-surface expression might provide a cure for NDI patients.

G protein-coupled receptors; endoplasmic reticulum; Madin-Darby canine kidney cells; protein degradation

TO INCREASE RENAL WATER REABSORPTION in states of hypernatremia or hypovolemia, pituitary-released arginine-vasopressin (AVP) binds to its vasopressin V2 receptor (V2R) in the basolateral membrane of polarized principal cells. This interaction induces the binding, activation, and cleavage of a trimeric Gs protein, of which the stimulatory α_s-subunit activates adenylate cyclase to generate cAMP. Through several steps, this eventually redistributes aquaporin-2 (AQP2) water channels from intracellular vesicles into the apical membrane, rendering this membrane permeable to water. Following an osmotic gradient over the epithelium, water can then be reabsorbed from the prourine to the blood.

In the rare inheritable disorder nephrogenic diabetes insipidus (NDI), patients are unable to concentrate their urine in response to AVP, resulting in the excretion of large volumes of dilute urine. Mutations in the *AVPR2* gene have shown to be causative for ~90% of all NDI cases and are inherited in an X-linked fashion. Autosomal NDI, either recessive or dominant, accounts for the remaining 10% of cases and is caused by mutations in the *AQP2* gene (10). To date, over 180 mutations have been described in the *AVPR2* gene, most of them being missense mutations.

Because an effective treatment of patients depends on the cellular defect introduced by the mutation, Zeitlin (27) classified mutations of the cystic fibrosis transmembrane conductance regulator gene into five different classes according to their cellular fate. Recently, we adapted this classification to G protein-coupled receptors in general and the V2R in particular (5). In this classification, class I mutations lead to defects in the synthesis of stable mRNA, resulting in the absence of protein. Promoter alterations, aberrant splicing, exon skipping, and most frame-shift and nonsense mutations fall into this category. Class II mutations lead to fully translated proteins, but they are trapped in the endoplasmic reticulum (ER), as they are misfolded. Class III mutants are normally transported to their site of action, but at that location they are disturbed in their activation or regulation. For the V2R, mutations on the cytosolic side of the protein that interfere with G protein binding and thus prevent intracellular signaling, like the R137H mutation (22), fall into this category. Class IV mutations also do not affect protein trafficking, but they impair or decrease the receptor's ability to bind ligand, as has been reported for V2R-ΔR202 (1) and V2R-R181C (19). Finally, class V mutations lead to proteins that are not disturbed in any of the above ways but are missorted to another organelle in the cell.

Knowledge of the cellular and molecular cause of mutant proteins in diseases is essential for the development of rationally based treatment. To prevent laborious cell biological analyses of all mutants, a prediction of the cellular fate of the mutant protein made on the basis of the identified mutation would be useful. However, for mutant proteins in general and the V2R in particular, it is at present unclear whether particular amino acid substitutions or locations of the mutations within the protein make the mutant likely to be of a particular class. In

Address for reprint requests and other correspondence: P. M.T. Deen, 160 Dept. of Physiology, NCMLS, Radboud Univ. Nijmegen Medical Ctr., PO Box 9101, 6500 HB Nijmegen, The Netherlands (e-mail: p.deen@ncmls.ru.nl).

The costs of publication of this article were defrayed in part by the payment of page charges. The article must therefore be hereby marked "*advertisement*" in accordance with 18 U.S.C. Section 1734 solely to indicate this fact.

addition, most data on the cellular cause of V2R mutants in NDI have been obtained from transiently transfected cells. Although possibly useful, these cells are not polarized, as renal principal cells, and proteins may rout differently from polarized cells (13). Moreover, due to the high expression levels in transient assays, the mutants are often expressed at several sites, which make interpretation of the proper cellular location difficult. Recently, we generated a Madin-Darby canine kidney (MDCK) cell line in which exogenous V2R is expressed and regulated by dDAVP as can be anticipated for the V2R in vivo (21). To address the issues above, we selected nine V2R mutations that cause NDI and are distributed along the V2R protein. Subsequently, we stably expressed these V2R mutants in MDCK cells and thoroughly analyzed their functionality, localization, degradation pathway, and stability.

MATERIALS AND METHODS

Materials. MG-132 was from Calbiochem (La Jolla, CA); chloroquine diphosphate, cycloheximide, IBMX, and dDAVP were from Sigma (St. Louis, MO). The pEGFP-N1-V2R plasmid encoding wild-type (wt)-V2R, COOH terminally tagged with the green fluorescent protein (GFP) (25), was kindly provided by Dr. Alexander Oksche (FMP, Berlin, Germany).

Expression constructs. With a three-step PCR reaction or quick-change site-directed mutagenesis kit (Stratagene, Heidelberg, Germany), each mutation was introduced into the human V2R cDNA sequence using pEGFP-N1-V2R as a template. Primers used were CGCTGCCATCCATAGTCTTTGTGG for L44P, CTGGTGCTGGCGGCCCGGGGCCGGCGGGG for Δ62–64, CCTGTGTTGGGCCGTGAAGTATC for R113W, GCCTCCTCCTACATGTTCCTGGC for I130F, CCTTCACACTCCTTCTCAGCCTGC for S167T, CCTTCTTGCTCCTTCTCAGCCTGC for S167L, CTGGGATCGTCGCACCTATGTCAC for G201D, GTCGCAACTATGTCACCTGGATTGC for T204N, and GTCGCACCTATGATACCTGGATTGC for V206D, and their complementary antisense primers. After digesting correct clones with *Bgl*II/*Pst*I (L44P, Δ62–64, R113W) or *Pst*I/*Hin*dIII (I130F, R137H, S167T, S167L, G201D, T204N and V206D), the mutation-containing fragments were isolated and cloned into the corresponding sites of wt-V2R-GFP. Sequence analysis of selected clones confirmed that only the desired mutations were introduced.

MDCK cells. MDCK cells were maintained and stably transfected, and immunocytochemistry and confocal laser-scanning microscopy (CLSM) were performed as described (7). As primary antibodies, 1:100-diluted rabbit anti protein disulfide isomerase (PDI; a kind gift of Dr. I. Braakman, Utrecht, The Netherlands); 1:200-diluted mouse anti-lysosome-associated membrane protein 2 (LAMP-2) antibodies (15), a kind gift of Dr. Le Bivic, Marseille, France; or 1:100-diluted rat anti E-cadherin (Sigma) were used. As secondary antibodies, 1:100-diluted goat anti-rabbit, goat anti-rat, or goat anti-mouse IgGs, all three coupled to Alexa 594, were used (Molecular Probes, Leiden, The Netherlands). Semiquantification of colocalization of V2R with cellular markers was done as described (21).

Stability and degradation experiments. To determine receptor stability, cell lines were incubated for either 0, 2, 4, or 8 h in culture medium containing 50 μM cycloheximide to block protein synthesis, after which the cells were lysed in 1× Laemmli sample buffer and subsequently analyzed by immunoblotting. To determine the degradation pathway of the receptors, cells were incubated in culture medium containing 50 μM cycloheximide, supplemented with 20 μM MG-132, 100 μM chloroquine, or both. Cells incubated in normal culture medium were used as controls. After 8 h, cells were lysed in 1× Laemmli sample buffer and subsequently analyzed by immunoblotting.

Immunoblotting. Protein samples were prepared and analyzed on a 10% polyacrylamide gel and subsequently blotted as described (7). For detection of V2R-GFP, 1:5,000-diluted rabbit anti-GFP antiserum (3) (kindly provided by Dr. B. Wieringa, UMCN, Nijmegen, The Netherlands) or 1:20,000 mouse anti-β-actin (Sigma) was used. As secondary antibodies, goat anti-rabbit or sheep anti-mouse IgGs coupled to horseradish peroxidase (Sigma) were used at a 1:5,000 dilution. Immunoblot signals were semiquantified using Image-Pro software (Media Cybernetics, Silver Spring, MD) as described (21). Data of at least three experiments were used for quantification.

cAMP measurement, [^{3}H]AVP binding, and cell-surface biotinylation. COS-M6 cells were seeded on six-well plates and grown to 80% confluence. Subsequently, 5 μg plasmid DNA encoding either wt or mutant V2R-GFP were transfected into the cells using lipofectamine. The next day, cells were seeded at 80% confluence and grown overnight in DMEM with 10% fetal calf serum in a humidified 37°C incubator under 5% CO_2. The cells were subsequently treated with prewarmed medium containing 100 nM dDAVP for 5 min in the absence of IBMX. After the cells were washed briefly in prewarmed PBS-CM, the cells were lysed in 100 μl of 0.1 M HCl, and cAMP was measured using a fluorescent cAMP assay kit (Sigma) according to the manufacturer's protocol. Assay plates were read in the Model 3550-UV Microplate Reader (Bio-Rad, Hercules, CA) using an excitation wavelength of 405 nm. Measurements were performed at least in triplicate.

For radioligand binding assays, transfected COS-M6 cells were grown overnight, seeded at a density of 5.0×10^5 cells/cm^2 on 12-well plates, and again grown overnight. Radioligand labeling was performed as described (21). Averaged data of at least three independent experiments were used.

For cell-surface biotinylation, transfected COS-M6 cells were grown for 2 days and subsequently biotinylated as described (7). Instead of filters, COS-M6 cells were grown on plastic supports.

Statistical analyses. All statistical analyses were calculated using MS Excel. The spread of values is indicated as SD. Significance was calculated by performing Student's *t*-test.

RESULTS

Localization of the V2R mutants. The nine V2R mutations, i.e., L44P, R113W, S167L, T204N, V206D (11), Δ62–64 (2), I130F (20), S167T (17), and G201D (23), which are dispersed over the V2R protein (Fig. 1), have been shown to cause NDI. In MDCK type I cells, the localization, maturation, and dDAVP-induced internalization of V2R-GFP mimic that anticipated for V2R in principal cells to a great extent (21). Therefore, we stably transfected MDCK cells with expression constructs encoding the V2R-GFP mutants mentioned. Multiple positive clones were isolated for each mutant. Immunocytochemistry and subsequent confocal laser-scanning microscopic analysis of V2R-S167L and -I130F showed a nearly complete colocalization with the ER marker PDI (Fig. 2, *top*). Semiquantification revealed a colocalization of 94.1 ± 4.5 and 94.3 ± 4.2%, respectively. The mutants V2R-L44P (92.4 ± 5.1%), -Δ62–64 (94.4 ± 3.4%), -S167T (92.3 ± 3.9%), and -V206D (95.7 ± 3.6%) showed similar results (not shown).

Confocal analysis of V2R-R113W and -G201D (Fig. 2, *middle*), however, showed only a partial colocalization with the ER marker PDI (53.3 ± 5.5 and 50.3 ± 8.5%, respectively). The remainder colocalized with the basolateral marker E-cadherin in the lateral membrane (44.8 ± 6.9 and 46.1 ± 8.1%, respectively) or with the late endosomal/lysosomal marker LAMP-2 (4.2 ± 2.4 and 5.6 ± 3.1%; not shown). Similar results were obtained for V2R-T204N (51.3 ± 7.9% with PDI; 43.2 ± 5.1% with E-cadherin; 5.1 ± 2.3% with LAMP-2; not shown). As reported (21), wt-V2R was expressed predominantly in the lateral plasma membrane of MDCK cells (75%), and to a lesser extent in late endsomes/lysosomes (25%), and

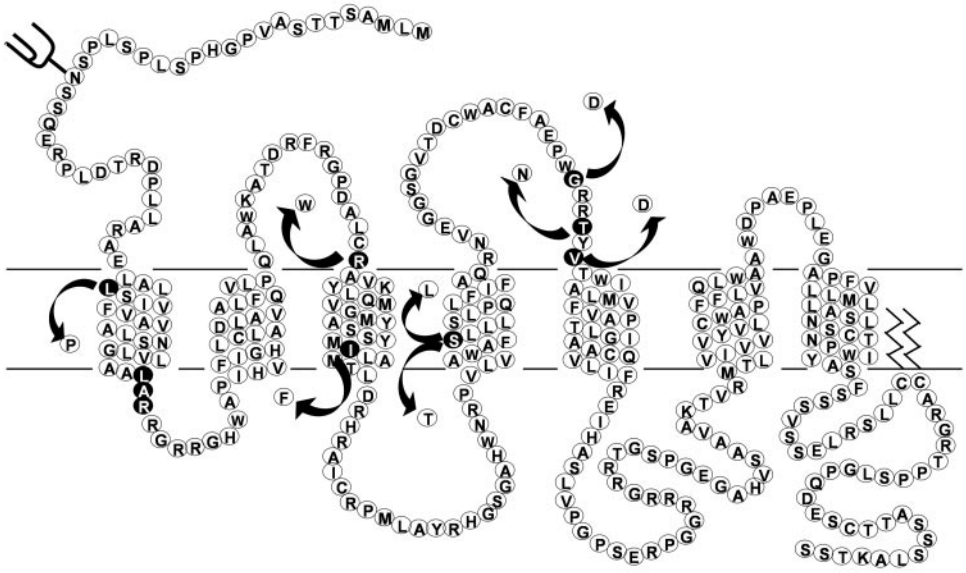

Fig. 1. Location of mutations in vasopressin V2 receptor (V2R) protein. Topological map of the human V2R is shown. Mutated residues are indicated in black; introduced amino acids are indicated by arrows.

did not show any colocalization with the ER marker protein (Fig. 2, *bottom*).

Maturation state of the V2R mutants. To test the maturation states of the different V2R mutants, total cell lysates were undigested, digested with endoglycosidasde H (Endo H), which removes N-linked high-mannose sugar groups, or with PNGase F, which removes all N-linked sugar moieties, and immunoblotted. Recently, we have reported that V2R-GFP is mainly expressed as complex-glycosylated proteins of 75 kDa (Fig. 3, *bottom*) (21). With Endo H, the majority remained unaffected, whereas some 60-kDa core-glycosylated V2R appeared. With PNGase F, the 75-kDa band was reduced to 67 kDa, which might represent O-glycosylated V2R.

Western blot analysis of undigested V2R-S167L (Fig. 3, *top left*) showed a strong 60-kDa core protein and a second band of ~63 kDa. This latter band disappeared with Endo H (and PNGase F) digestion, which indicated that this band represents high-mannose glycosylated V2R-GFP. These data suggested that most, if not all, V2R-S167L is retained in the ER. Similar results were obtained for V2R-L44P, -Δ62–64, -S167T, and -V206D (not shown).

V2R-I130F was also mainly expressed as 60- and 63-kDa bands, although weak bands of 67 and 75 kDa were observed (Fig. 3, *top right*). Upon digestion with Endo H, the weak 75-kDa and strong 60-kDa bands remained, whereas a faint band of ~65 kDa appeared. The 63-kDa band disappeared with Endo H. With PNGase F, a weak 67-kDa band and strong 60-kDa band were observed. The presence of the weak 75-, 65-, and 67-kDa bands indicated that a small fraction of V2R-I130F has left the ER and was partially (65

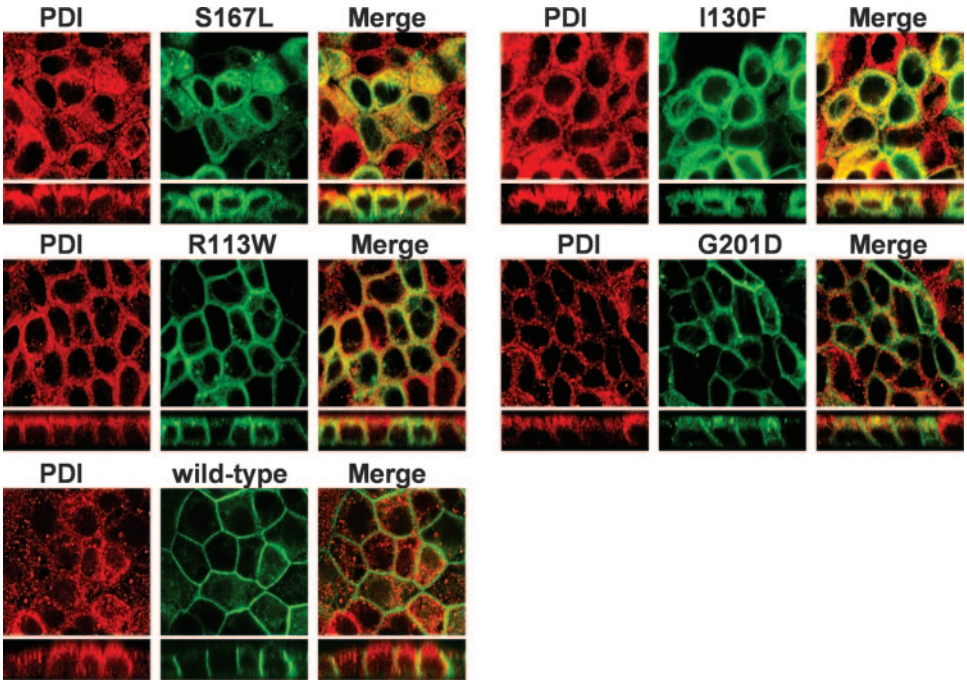

Fig. 2. Localization of nephrogenic diabetes insipidus (NDI) causing V2R mutants. Madin-Darby canine kidney (MDCK) cell lines stably expressing V2R-S167L, -I130F, -R113W, -G201D, or wild-type V2R were grown to confluence and fixed. Immunocytochemistry was done for protein disulfide isomerase (PDI) to stain the endoplasmic reticulum (ER). Signals for PDI and the V2R are shown in red and green, respectively.

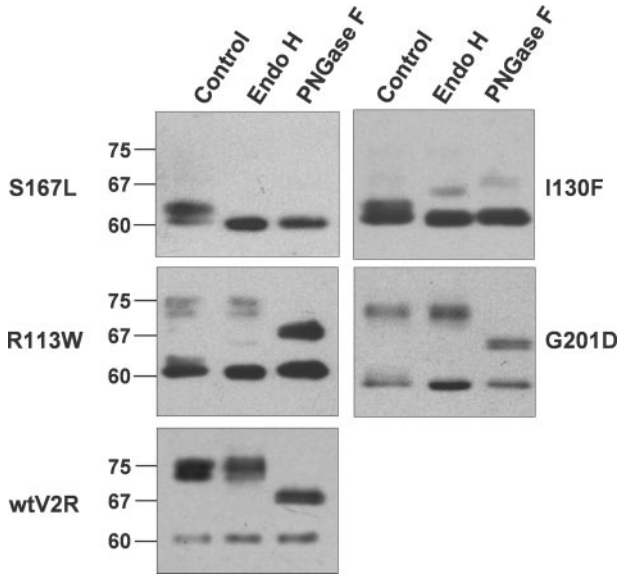

Fig. 3. Maturation of NDI causing V2R mutants. To determine the glycosylation state of V2R-S167L, -I130F, -R113W, -G201D, or wild-type (wt)-V2R (indicated), confluent MDCK-V2R-green fluorescent protein (GFP) cells were lysed in Laemmli buffer, treated without any enzyme (control), or with Endo H or PNGase F, and analyzed by immunoblotting using anti-GFP antibodies. Estimated masses (in kDa) are given on the *left*.

kDa with Endo H) or fully (75 kDa; 67 kDa with PNGase F) matured.

Analysis of the maturation of V2R-R113W revealed similar bands as those observed for V2R-I130F, except here the bands of 75 (control and endo H) and 67 (PNGase F) kDa were stronger for V2R-R113W (Fig. 3, *middle left*). V2R-G201D was even more mature, because the 75- and 67 (PNGase F)-kDa bands were of similar intensity as the core form (Fig. 3, *middle right*). Similar data as for V2R-G201D were obtained for V2R-T204N (not shown). Semiquantification of the signals confirmed the differences in maturation, because data for V2R-I130F, -R113W, -G201D, and -T204N show that 7.3 ± 4.1, 59.2 ± 5.9, 64.3 ± 7.1, and 66.6 ± 4.5% were expressed as 75-kDa proteins, respectively ($n = 3$), whereas the remainder comprises core- and high-mannose glycosylated proteins. These data demonstrate that the mutants V2R-R113W, -G201D, and -T204N are only partially retained in the ER and that a considerable proportion undergoes maturation. Similar patterns were observed for transfected clones with different expression levels of these mutants (not shown), indicating that the observed differences in maturation were related to the mutation and not due to clonal differences in expression levels.

Stability of V2R mutants. As introduced mutations may affect the stability of proteins, we determined the half-lives ($t_{1/2}$) of the V2R mutants. Following a protein synthesis block with cycloheximide, the total V2R content of the cells was monitored over time. V2R-S167L (Fig. 4, first panel) showed a rapid decrease in its 60/63-kDa bands (here, they run as 1 band). Semiquantification of the signals ($n = 3$) revealed a $t_{1/2}$ of 1.5 ± 0.4 h for V2R-S167L. The $t_{1/2}$ of V2R-L44P (1.5 ± 0.3 h), -S167T (2.4 ± 0.4 h), and -V206D (3.2 ± 0.7 h) were in the same range (not shown). The 60/63-kDa bands of V2R-Δ62–64, however, were much more stable, as it has a calculated $t_{1/2}$ of 12.5 ± 3.4 h (Fig. 4, second panel). The mutant V2R-I130F (Fig. 4, third panel) also showed a rapid decrease in its 60/63-kDa bands, from which we calculated a $t_{1/2}$ of 1.9 ± 0.5 h. We were not able to quantify the stability of V2R-I130F's complex-glycosylated form, as this signal was too weak for this analysis.

As V2R-R113W, -G201D, and -T204N are expressed as core-glycosylated (60/63 kDa) and complex-glycosylated (75 kDa) proteins, we analyzed the stability of both forms. Semiquantification revealed that complex-glycosylated V2R-R113W had a $t_{1/2}$ of 14.4 ± 3.2 h. In contrast, the 60/63-kDa form had a $t_{1/2}$ of only 2.1 ± 0.3 h. For V2R-G201D, the $t_{1/2}$of the complex-glycosylated form was only 4.1 ± 1.5 h. Although a rapid decrease is observed during the first 2 h for the high-mannose glycosylated V2R-G201D, hardly any degradation is observed beyond this period, leading to a calculated $t_{1/2}$ of 10.2 ± 3.0 h. For V2R-T204N, the $t_{1/2}$ of the complex-glycosylated form and the high-mannose glycoyslated form were 2.2 ± 0.6 and 2.1 ± 0.2 h, respectively (Fig. 4, sixth panel). Again, similar $t_{1/2}$ were obtained from two independent clones per construct, indicating that the differences in $t_{1/2}$ are not due to clonal differences. As reported, wt-V2R has a $t_{1/2}$ of 11.5 ± 2.8 h (21).

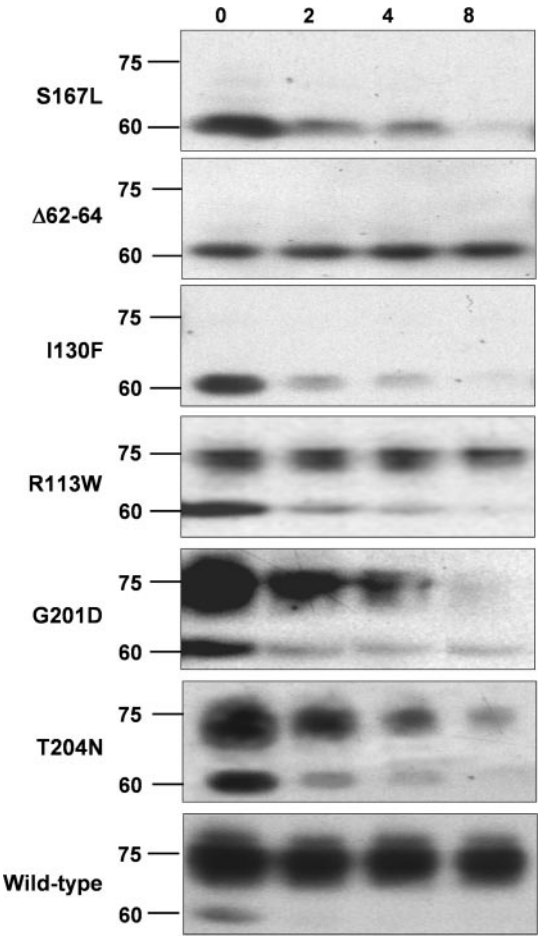

Fig. 4. Stability of NDI causing V2R mutants. MDCK cells expressing V2R-S167L, -Δ62–64, -I130F, -R113W, -G201D, -T204N, or wt-V2R were grown to confluence and subsequently treated with 50 μM cycloheximide to block protein synthesis. At the indicated time points (h), cells were lysed in Laemmli sample buffer and analyzed by immunoblotting as indicated in the legend for Fig. 3. Estimated masses (in kDa) are given on the *left*.

Degradation pathway of the V2R mutants. Proteins can be degraded by the proteasomal pathway, which can be inhibited by MG-132, or the lysosomal pathway, which is inhibited by chloroquine and, sometimes, MG-132. Considering the differences in stability of the mutants, we next studied their degradation pathways by incubating the cells for 8 h with cycloheximide alone or combined with MG-132, chloroquine, or both. As shown in Fig. 5 (first and second panels), the degradation of V2R-S167L and -I130F was nearly completely prevented by MG-132, whereas chloroquine had no effect on its own, nor in combination with MG-132. Similar results were obtained for the mutants V2R-L44P, -Δ62–64, -S167T, and -V206D (not shown).

The degradation of the complex-glycosylated bands of V2R-R113W was partially prevented by coincubation with either chloroquine or MG-132 (Fig. 5, third panel). Incubation with both inhibitors revealed no degradation at all. Strikingly, of the two most prominent bands of complex-glycosylated V2R-R113W, chloroquine stabilized the larger form, whereas MG-132 treatment mainly prevented degradation of the lower band. The 60/63-kDa band was only partially prevented from degradation by the combination of MG-132 and chloroquine.

For V2R-G201D (Fig. 5, fourth panel), chloroquine treatment did not prevent degradation of the high-mannose or complex-glycosylated form. MG-132, however, prevented degradation of both, resulting in similar protein levels as found in the untreated sample. Combined treatment of chloroquine and MG-132 did not show an additional effect compared with MG-132 alone. For V2R-T204N (Fig. 5, fifth panel), cycloheximide treatment resulted in decreased V2R protein levels of both the complex- and the 60/63-kDa forms. Chloroquine treatment completely prevented degradation of the complex-glycosylated form of V2R-T204N but did not prevent degradation of the 60/63-kDa forms. MG-132 partially prevented the degradation of the complex-glycosylated form (~14%), and completely prevented the degradation of the 60/63-kDa forms of the V2R-T204N. Combined MG-132/chloroquine treatment did not result in >60/63-kDa or complex-glycosylated V2R-T204N compared with MG-132 or chloroquine alone. Degradation of the complex-glycosylated form of the wt-V2R (Fig. 5, fifth panel) could completely be prevented by cotreatment with chloroquine, whereas MG-132 was able to prevent degradation of the high-mannose glycosylated form.

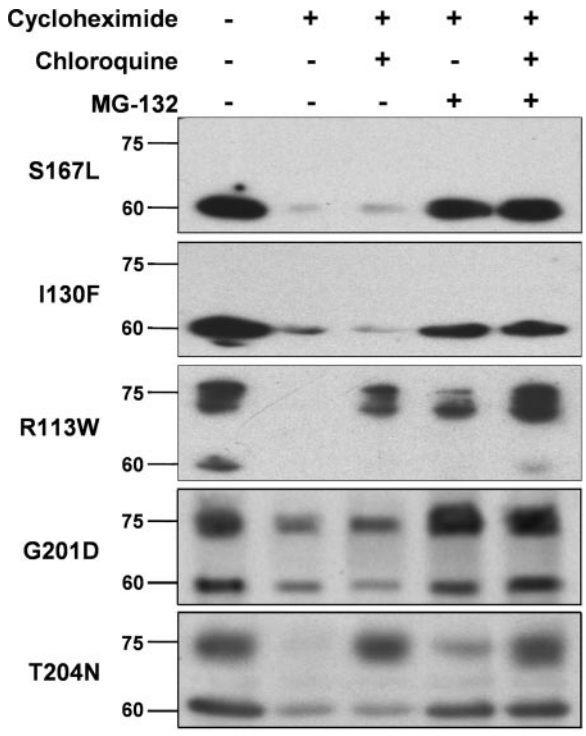

Fig. 5. Degradation pathways of NDI causing V2R mutants. Cell lines stably expressing V2R-S167L, -I130F, -R113W, -G201D -T204N, or wt-V2R were treated for 8 h as indicated. Western blot analysis was performed as described in the legend for Fig. 3. Estimated masses (in kDa) are given on the *left*.

Receptor functionality. To assess which V2R mutants are functional, the mutant's ability to generate cAMP in response to a dDAVP treatment was determined. As MDCK type I cells express low levels of endogenous V2R (6, 21), receptor functionality assays were performed in COS cells, as these cells do not endogenously express V2Rs. Furthermore, to obtain some mutant receptor expressed at the cell surface, these cells were transiently transfected, as this mostly gives high expression levels. As shown in Fig. 6*A*, dDAVP binding of the mutants V2R-L44P, -R113W, -I130F, -S167T, -G201D, and -T204N resulted in significantly increased cAMP levels compared with mock-transfected cells ($P < 0.001$; $n = \geq 3$), indicating that these mutants can translate AVP binding into a cAMP response. The mutants V2R-Δ62–64, -S167L, and -V206D showed no significant cAMP increase compared with mock-transfected cells. Because the expression of these three mutants was similar to or greater than that of functional V2R-S167T (Fig. 6*B*) and they have similar localizations and maturation characteristics (Figs. 2 and 3), these three mutants were likely to be interfered with in their binding to dDAVP or activating a Gs protein.

To investigate this further, COS cells expressing V2R-GFP, V2R-Δ62–64, -S167L, -V206D, and the functional mutants V2R-L44P or -I130F were subjected to radioligand binding assays. As shown in Fig. 6*C*, V2R-L44P, -I130F, and -Δ62–64 bind significantly more [^{3}H]AVP than mock-transfected cells ($P < 0.001$; $n = \geq 3$). No significant binding was observed for cells expressing V2R-S167L and -V206D ($P > 0.05$; $n = \geq 3$). V2R-GFP-expressing cells bound radioligand to 19,619 ± 2,453 counts (not shown).

Because the lack of AVP binding and cAMP generation could be due to the lack of expression in the plasma membrane, transfected COS cells were subjected to cell-surface biotinylation assays. Immunoblotting of the obtained samples, however, revealed that the plasma membrane expression levels of the non-AVP binding receptors V2R-S167L and V2R-V206D were clearly higher than that of the functional V2R-L44P (Fig. 6*D*). In these biotinylation samples, no signals for β-actin were observed (Fig. 6*D*, *bottom*), whereas strong actin signals were obtained in the corresponding lysate sample of COS cells expressing wt-V2R (Fig. 6*D*) or the mutants (not shown). This indicated that the biotinylation samples did not contain intracellular proteins. Therefore, these data reveal that V2R-S167L and V2R-V206D are unable to generate an intracellular cAMP response due to their inability to bind AVP.

DISCUSSION

All V2R mutants are retained in the ER, but at different levels. To study the cellular fate (summary in Table 1) of nine V2R mutants involved in NDI, MDCK cells were stably

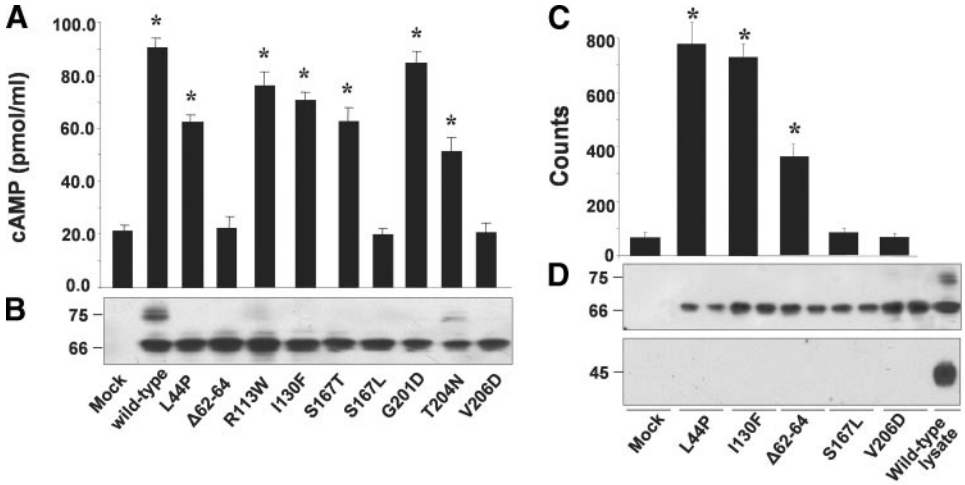

Fig. 6. Functionality of NDI causing V2R mutants. *A*: cAMP generation. COS-M6 cells transiently expressing either wt-V2R or mutant V2R proteins were treated for 5 min with 100 nM dDAVP, washed in PBS-CM, and lysed in 0.1 M HCl, followed by cAMP measurement in a fluorescence-based assay. *Significantly different from mock-transfected cells ($P < 0.001$); $n = \geq 3$. *B*: V2R protein expression levels. Cell equivalents from the experiment in *A* were lysed in Laemmli buffer and subjected to immunoblotting as described in the legend for Fig. 3. *C*: AVP binding. Transiently transfected COS cells were incubated for 1 h at 4°C with 100 nM [^{3}H]AVP in PBS-CM followed by washing, scraping, and counting in a scintillation counter. *Significant difference in radioligand binding compared with mock-transfected cells ($P < 0.01$); $n = 3$. *D*: cell-surface expression of V2R proteins. Transiently transfected COS cells from *C* were subjected to cell-surface biotinylation. Cell-surface proteins were subjected to immunoblotting for V2R (*top*) or β-actin (*bottom*) as described in the legend for Fig. 3. As a control for the antibodies, the *far right* lane contains a total lysate sample of COS cells expressing wt-V2R.

transfected with expression constructs for these proteins. CLSM analysis revealed that all mutants colocalized with the ER marker protein PDI, indicating their retention in the ER. The level of ER retention, however, differed among mutants. Whereas the mutants V2R-L44P, -Δ62–64, -S167T, -S167L, and -V206D were restricted to the ER (*group 1*), a considerable fraction of V2R-R113W, -G201D, and -T204N was expressed in the basolateral membrane (*group 2*; Fig. 2). Their level of maturation was consistent with the observed localizations, as the members of *group 1* were only expressed as nonglycosylated 60-kDa or core-glycosylated 63-kDa proteins, whereas the *group 2* receptors were expressed as immature 60/63-kDa proteins and mature complex-glycosylated proteins (Fig. 3). Pronounced ER retention has also been reported for V2R-Δ62–64 and -S167L in HEK293 cells (9) and for the V2R mutants L292P, ΔV278, and R337X in polarized MDCK cells (26).

An exception is formed by V2R-I130F, which seemed restricted to the ER with immunocytochemistry, but of which immunoblot data of Endo H or PNGase F digestions revealed a small fraction of intermediate or complex-glycosylated receptor. Of V2R-I130F, only 7.3% is expressed in a mature form, whereas 60–70% of V2R-R113W, -G201D, and -T204N is expressed in the mature form. Therefore, mature V2R-I130F may possibly be present in the basolateral membrane at levels that could not be detected by immunocytochemistry. Taken together, these data indicate that the level of ER retention and maturation of V2R-I130F is in between that of the two groups.

Our finding that all mutants are, at least partially, retained in the ER illustrates the high sensitivity of the ER quality control mechanism to identify mutant proteins. Strikingly, based on the proposed topology of the V2R (24), all V2R mutations leading to strong ER retention are located in either one of the transmembrane domains (TMD; L44P, I130F, S167T, S167L) or change a hydrophobic into a charged amino acid at the edge of a TMD (L into R in V2R-Δ62–64, V206D). These mutations might interfere with the proper folding or positioning of the hydrophobic TMDs, of which luminal or cytosolic exposure is thought to render proteins prone to recognition by the ER quality control mechanism, ER retention, and subsequent degradation (8, 12). The slightly better maturation of V2R-I130F compared with the others might be due to an exchange of a hydrophobic amino acid for another in the TMD of V2R-I130F. In contrast, with V2R-

Table 1. *Localization, maturation, functionality, and classification of wild-type and mutant V2R*

	L44P	Δ62–64	S167T	S167L	V206D	I130F	R113W	G201D	T204N	wt-V2R
Location of mutation	TM I	ICL 1	TM IV	TM IV	ECL 2	TM III	ECL 1	ECL 2	ECL 2	NA
Cellular localization	ER	ER	ER	ER	ER	ER	ER, PM, LE	ER, PM, LE	ER, PM, LE	PM, LE
Glycosylation	HM	HM	HM	HM	HM	HM/(C)	HM/C	HM/C	HM/C	C
Half-life, h	1.5	12.5	2.4	1.5	3.2	1.9	2.1/14.4	10.2/4.1	2.1/2.2	11.5
Degradation	MS	MS	MS	MS	MS	MS	MS/CS	MS/CS	MS/CS	CS
AVP binding	+	+	NA	−	−	+	NA	NA	NA	+++
cAMP response	+	−	+	−	−	+	++	+++	++	+++
Mutant class	II	II	II	II	II	II	II and IV	II and IV	II and IV	

Shown is a summary of the data from Figs. 1–6. V2R, vasopressin V2 receptor; TM, transmembrane domain; ICL, intracellular loop; ECL, extracellular loop; PM, plasma membrane; LE, late endosomes and lysosomes; ER, endoplasmic reticulum; C, complex-glycosylated; HM, high-mannose glycosylated; MS, MG132-sensitive degradation; CS, chloroquine-sensitive degradation; wt, wild-type; NA, nonapplicable. Mutants were classified according to Deen et al. (5).

L44P, the introduced proline is likely to introduce a knick and therefore distort the α-helical structure of TMDI.

Our finding that V2R mutants, mutations of which are located in the third extracellular loop (G201D and T204N) or introduce a hydrophobic amino acid at the edge of the first extracellular loop and TMD III (R113W), suggests that mutations located on the ER luminal side of V2R are causing less severe misfolding of the receptor protein compared with mutations in the TMD. Alternatively, they might be less well recognized by ER quality control proteins than transmembrane or cytosolic segments. Definite answers to these issues can only be given when the atomic structure of the V2R has been elucidated.

Stability and degradation of V2R mutants. To further study the fate of the V2R mutant proteins, their stability and degradation pathways were investigated (Figs. 4 and 5; Table 1). Compared with the $t_{1/2}$ of complex-glycosylated wt-V2R, the stability of ER-retained mutants in general was drastically reduced (up to 8.5-fold). Also, degradation of the ER-retained V2R forms (60/63 kDa) occurred for most mutants through the proteasomal pathway, as MG-132, which interferes with proteolysis by the proteasome, greatly stabilized most 60/63-kDa V2R mutants. These data are consistent with the current view that wt or mutant proteins targeted for degradation from the ER are processed via the so-called ER-associated degradation (ERAD) pathway, which involves the recognition of misfolded proteins by molecular chaperones, their transport from the ER to the cytoplasm through an ER translocon, and degradation in the cytosol by proteasomes. V2R-G201D and V2R-Δ62–64 seem to form exceptions to this rule. Although a considerable portion of the 60/63-kDa V2R-G201D proteins was degraded within 2 h, a small fraction appeared very stable (8 h; Fig. 5). This might indicate that, whereas most V2R-G201D is recognized as misfolded and degraded, a small portion might be resistant to recognition by molecular chaperones, transport from the ER and/or degradation by proteasomes. More interesting, however, the $t_{1/2}$ of V2R-Δ62–64 was similar to that of wt-V2R. Because this is the only mutant in which amino acids are deleted instead of exchanged, it might suggest that the ERAD pathway is more sensitive to missense mutations than to a lack of amino acids. Alternatively, because we only studied one deletion mutant, the difference might be just coincidental. Therefore, analysis of more V2R deletion mutants is required to address this issue.

For the complex-glycosylated forms of the mutants (i.e., V2R-R113W, -G201D, -T204N), the stability and degradation pathways vary considerably and appear unrelated to the stability and degradation pathways acting on the immature receptors. Mature V2R-GFP was degraded only by the proteasomal pathway, as only chloroquine inhibited its degradation. V2R tagged at its NH_2 terminal with an HA tag showed a similar stability ($t_{1/2}$ = 12.2 ± 3.8 h) and degradation pathway to V2R-GFP (not shown), which indicated that neither the tag (GFP or HA) nor its site of coupling (NH_2 or COOH terminal) affected V2R degradation. This was different for the V2R mutants. While V2R-T204N is also only degraded by the lysosomal pathway, V2R-R113W degradation was inhibited by MG-132 and chloroquine, whereas V2R-G201D degraded was only inhibited by MG-132. These results might indicate that mutations that are located at the luminal side of the membrane can induce the degradation of mature V2R by proteasomes, which are thought to degrade proteins from the cytosolic side. Alternatively, these V2R mutants are also degraded in lysosomes, as MG-132 is also a highly potent inhibitor of various cysteine proteases and cathepsins (29, 30). The degradation pathway used for the mature mutants, however, does not appear to be indicative of their stability, because V2R-G201D and V2R-T204N are three to six times less stable than wt-V2R, whereas mature AQP2-R113W is as stable as wt-V2R. Complex-glycosylated proteins are formed from core-glycosylated proteins in the Golgi complex and, therefore, the observed stabilities of the V2R proteins might be overestimated. Along the same line, the observed high stability of V2R-R113W compared with V2R-G201D and -T204N might be due to a higher level of immature V2R-R113W processed through the Golgi complex. Although this cannot be excluded, the similar or low stability of immature V2R-R113W compared with those of V2R-G210D and -T204N render this possibility rather unlikely. More likely, the observed differences are due to different impacts of the mutations on the structure of the V2R. How mature V2R mutants are targeted for proteasomal and/or lysosomal degradation, however, remains unclear.

Functionality of V2R mutants. All mutants tested, with the exception of V2R-Δ62–64, -S167L, and -V206D, showed significantly increased cAMP levels compared with nontransfected COS cells in a transient overexpression system and were thus designated as being functional. Of the "non-functional" mutants, only V2R-Δ62–64 was able to bind AVP. V2R-S167L and -V206D did not bind detectable levels of AVP, although their membrane expression levels were higher than that of the AVP-binding mutant V2R-L44P, which indicated that the lack of V2R-S167L and -V206D to mediate a cAMP response is due to a reduced ability to bind AVP. In contrast to our study, Morello et al. (14) found a cAMP response with rescued V2R-Δ62–64. This discrepancy might be caused by their use of the PDE inhibitor IBMX, their 100-fold higher dDAVP concentration, the longer cAMP accumulation time (20 vs. 5 min here), and/or increased expression of this mutant receptor due to its rescue to the cell surface by the V2R antagonist SR121463A. Both data, however, are in line with the hypothesis of Oksche et al. (16) that the first intracellular loop of the V2R is involved in Gs protein binding and that this is greatly reduced by the Δ62–64 mutation, thereby reducing the activation of adenylate cyclase. With the V2R-V206D mutant, there is a discrepancy between our data and the data from Postina et al. (20a), who observed a residual cAMP formation upon stimulation, but no AVP binding. Here, it might be due to the higher amount of DNA in their transient COS transfection experiments (~1 μg DNA/cm^2 compared with 0.5 μg DNA/cm^2), the presence of IBMX, the long incubation time with dDAVP (40 min compared with 5 min), and/or the higher dDAVP concentration used (1 μM). However, our data are consistent with the computer model of Czaplewski et al. (4), which hypothesizes that V206 is important for AVP binding.

Classification of mutations in the V2R. In line with our cell biological data, patients encoding V2R mutants that are severely ER retarded in our cell model (V2R with L44P, Δ62–64, I130F, S167T, S167L, V206D) do not increase their urine concentration in response to administration of dDAVP (2, 11, 18, 20). In contrast but consistent with the observed maturation and partial basolateral membrane expression in MDCK cells, patients encoding V2R-G201D (23) or -T204N (Knoers

NVAM, unpublished observations) are able to increase their urine concentrating ability on administration of a high dose of dDAVP. For patients carrying the R113W mutation, no increased urine concentrating ability after dDAVP administration has been reported. Overall, these parallels with in vivo findings provide further support that stably transfected polarized MDCK cells are a good model for the study of the cell biological features of wt and mutant V2R proteins.

In conclusion, our data reveal that all nine V2R mutations studied are of class II, because all V2R mutants studied are retained in the ER. The V2R-R113W, -G201D, and -T204N mutants, however, are also partially expressed in the basolateral membrane of MDCK cells and initiate a cAMP response following AVP binding, which reveals that these mutations are also of class IV. It has to be noted, however, that we cannot exclude the possibility that the mutations studied result in unstable V2R (pre-) mRNAs in vivo (i.e., class I mutations).

Recently, Morello et al. (14) showed that the cell-surface expression of several V2R mutants of class II could be rescued by cell-permeable V2R antagonists. Here, we found that all nine V2R mutations studied were of this class, of which six (L44P, R113W, I130F, S167T, G201D, T204N) turned out to be able to translate AVP binding into a cAMP response. Therefore, identifying cell-permeable pharmacological chaperones that are able to rescue these six mutants may eventually lead to a specific treatment to relieve NDI patients harboring functional class II V2R mutations from their disease.

ACKNOWLEDGMENTS

We thank Dr. A. Oksche (FMP, Berlin, Germany) for providing the V2R-GFP expression construct, Dr. B. Wieringa (Cell Biology, UMC Nijmegen, The Netherlands) for rabbit anti-GPF antiserum, Dr. I. Braakman (Utrecht, The Netherlands) for rabbit anti-PDI antibodies, and Dr. A. Le Bivic (Marseille, France) for mouse anti-LAMP-2 antibodies.

GRANTS

This project was supported by a grant from the Dutch Kidney Foundation (PC 104) to P. M. T. Deen and N. V. A. M. Knoers and from the European Union (QLK3-CT-2001–00987) to P. M. T. Deen.

REFERENCES

1. **Ala Y, Morin D, Mouillac B, Sabatier N, Vargas R, Cotte N, Dechaux M, Antignac C, Arthus MF, Lonergan M, Turner MS, Balestre MN, Alonso G, Hibert M, Barberis C, Hendy GN, Bichet DG, and Jard S.** Functional studies of twelve mutant V2 vasopressin receptors related to nephrogenic diabetes insipidus: molecular basis of a mild clinical phenotype. *J Am Soc Nephrol* 9: 1861–1872, 1998.
2. **Bichet DG, Birnbaumer M, Lonergan M, Arthus MF, Rosenthal W, Goodyer P, Nivet H, Benoit S, Giampietro P, and Simonetti S.** Nature and recurrence of AVPR2 mutations in X-linked nephrogenic diabetes insipidus. *Am J Hum Genet* 55: 278–286, 1994.
3. **Cuppen E, van Ham M, Wansink DG, de Leeuw A, Wieringa B, and Hendriks W.** The zyxin-related protein TRIP6 interacts with PDZ motifs in the adaptor protein RIL and the protein tyrosine phosphatase PTP-BL. *Eur J Cell Biol* 79: 283–293, 2000.
4. **Czaplewski C, Kazmierkiewicz R, and Ciarkowski J.** Molecular modeling of the human vasopressin V2 receptor/agonist complex. *J Comput Aided Mol Des* 12: 275–287, 1998.
5. **Deen PMT, Marr N, Kamsteeg EJ, and Van Balkom BWM.** Nephrogenic diabetes insipidus. *Curr Opin Nephrol Hypertens* 9: 591–595, 2000.
6. **Deen PMT, Rijss JPL, Mulders SM, Errington RJ, VanBaal J, and Vanos CH.** Aquaporin-2 transfection of Madin-Darby canine kidney cells reconstitutes vasopressin-regulated transcellular osmotic water transport. *J Am Soc Nephrol* 8: 1493–1501, 1997.
7. **Deen PMT, Van Balkom BWM, Savelkoul PJM, Kamsteeg EJ, van Raak M, Jennings ML, Muth TR, Rajendran V, and Caplan MJ.** Aquaporin-2: COOH terminus is necessary but not sufficient for routing to the apical membrane. *Am J Physiol Renal Physiol* 282: F330–F340, 2002.
8. **Ellgaard L and Helenius A.** ER quality control: towards an understanding at the molecular level. *Curr Opin Cell Biol* 13: 431–437, 2001.
9. **Hermosilla R, Oueslati M, Donalies U, Schonenberger E, Krause E, Oksche A, Rosenthal W, and Schulein R.** Disease-causing V2 vasopressin receptors are retained in different compartments of the early secretory pathway. *Traffic* 5: 993–1005, 2004.
10. **Knoers NV and Deen PM.** Molecular and cellular defects in nephrogenic diabetes insipidus. *Pediatr Nephrol* 16: 1146–1152, 2001.
11. **Knoers NVAM, Vandenouweland AMW, Verdijk M, Monnens LAH, and VanOost BA.** Inheritance of mutations in the V-2 receptor gene in 13 families with nephrogenic diabetes-insipidus. *Kidney Int* 46: 170–176, 1994.
12. **Ma Y and Hendershot LM.** The unfolding tale of the unfolded protein response. *Cell* 107: 827–830, 2001.
13. **Mellman I, Yamamoto E, Whitney JA, Kim M, Hunziker W, and Matter K.** Molecular sorting in polarized and non-polarized cells: common problems, common solutions. *J Cell Sci Suppl* 17: 1–7, 1993.
14. **Morello JP, Salahpour A, Laperriere A, Bernier V, Arthus MF, Lonergan M, Petaja-Repo U, Angers S, Morin D, Bichet DG, and Bouvier M.** Pharmacological chaperones rescue cell-surface expression and function of misfolded V2 vasopressin receptor mutants. *J Clin Invest* 105: 887–895, 2000.
15. **Nabi IR, Le Bivic A, Fambrough D, and Rodriguez-Boulan E.** An endogenous MDCK lysosomal membrane glycoprotein is targeted basolaterally before delivery to lysosomes. *J Cell Biol* 115: 1573–1584, 1991.
16. **Oksche A, Dehe M, Schulein R, Wiesner B, and Rosenthal W.** Folding and cell surface expression of the vasopressin V2 receptor: requirement of the intracellular C-terminus. *FEBS Lett* 424: 57–62, 1998.
17. **Oksche A, Dickson J, Schulein R, Seyberth HW, Muller M, Rascher W, Birnbaumer M, and Rosenthal W.** Two novel mutations in the vasopressin V2 receptor gene in patients with congenital nephrogenic diabetes insipidus. *Biochem Biophys Res Commun* 205: 552–557, 1994.
18. **Oksche A, Moller A, Dickson J, Rosendahl W, Rascher W, Bichet DG, and Rosenthal W.** Two novel mutations in the aquaporin-2 and the vasopressin V2 receptor genes in patients with congenital nephrogenic diabetes insipidus. *Hum Genet* 98: 587–589, 1996.
19. **Pan Y, Wilson P, and Gitschier J.** The effect of eight V2 vasopressin receptor mutations on stimulation of adenylyl cyclase and binding to vasopressin. *J Biol Chem* 269: 31933–31937, 1994.
20. **Pasel K, Schulz A, Timmermann K, Linnemann K, Hoeltzenbein M, Jaaskelainen J, Gruters A, Filler G, and Schoneberg T.** Functional characterization of the molecular defects causing nephrogenic diabetes insipidus in eight families. *J Clin Endocrinol Metab* 85: 1703–1710, 2000.

20a. **Postina R, Ufer E, Pfeiffer R, Knoers NV, and Fahrenholz F.** Misfolded vasopressin V2 receptors caused by extracellular point mutations entail congenital nephrogenic diabetes insipidus. *Mol Cell Endocrinol* 164: 31–39, 2000.

21. **Robben JH, Knoers NVAM, and Deen PMT.** Regulation of the vasopressin V2 receptor by vasopressin in polarized renal collecting duct cells. *Mol Biol Cell* 15: 5693–5699, 2004.
22. **Rosenthal W, Antaramian A, Gilbert S, and Birnbaumer M.** Nephrogenic diabetes insipidus—a V2 vasopressin receptor unable to stimulate adenylyl cyclase. *J Biol Chem* 268: 13030–13033, 1993.
23. **Sadeghi H, Robertson GL, Bichet DG, Innamorati G, and Birnbaumer M.** Biochemical basis of partial nephrogenic diabetes insipidus phenotypes. *Mol Endocrinol* 11: 1806–1813, 1997.
24. **Sadeghi HM, Innamorati G, Dagarag M, and Birnbaumer M.** Palmitoylation of the V2 vasopressin receptor. *Mol Pharmacol* 52: 21–29, 1997.
25. **Schulein R, Hermosilla R, Oksche A, Dehe M, Wiesner B, Krause G, and Rosenthal W.** A dileucine sequence and an upstream glutamate residue in the intracellular carboxyl terminus of the vasopressin V2 receptor are essential for cell surface transport in COS-M6 cells. *Mol Pharmacol* 54: 525–535, 1998.
26. **Tan CM, Nickols HH, and Limbird LE.** Appropriate polarization following pharmacological rescue of V2 vasopressin receptors encoded by X-linked nephrogenic diabetes insipidus alleles involves a conformation of the receptor that also attains mature glycosylation. *J Biol Chem* 278: 35678–35686, 2003.
27. **Zeitlin PL.** Novel pharmacologic therapies for cystic fibrosis. *J Clin Invest* 103: 447–452, 1999.